Supporting Information

Klimtchuk et al.

SI Materials and Methods

Clinical Data Collection. Demographic, clinical, and laboratory data were deposited in a database maintained by the Amyloidosis Center. Serum samples from the proband were obtained at the initial and two follow-up evaluations and stored at -20 °C prior to analysis, along with the control serum sample.

Analysis of Amyloid Deposits. Previously published proteomics methods were used for typing the amyloid deposits present in the formalin-fixed paraffin-embedded skin tissue biopsy (1). In brief, a 10-μM thick skin tissue section was cut and mounted on a special Director (OncoplexDX, Rockville, MD) slide. Section was stained with Congo red and mounted on a laser microdissection apparatus. Amyloid deposits were visualized under a fluorescent light and Congo red positive tissue fragments from an area of 60,000μM^2 were collected. Proteins in the collected fragments were extracted using heat and digested into peptides by incubating them overnight with trypsin. The peptide fragments were analyzed using either a QExactive or LTQ-Orbitrap mass spectrometer (Therm-Fisher Scientific, Waltham, MA),

The MS/MS data was processed using a previously published informatics pipeline (2). In brief, MS/MS were searched against SwissProt human reference database supplemented with reversed sequence entries to estimate protein and peptide identification probabilities. Two different search engines (Mascot and X!Tandem) were used to perform the peptide-spectrum matching and the results were processed using Scaffold software (Proteome Software, Portland, OR). Proteins with at least one confident identification probability ≥0.9 were utilized for interpretation. A pathologist inspected the detected proteins for presence of a universal amyloid signature and type specific proteins (3). The data were re-interrogated for known and unknown mutations in type specific proteins using a previously published pipeline (4).

Serum Screening, Genetic and Serum Protein Analyses. Isoelectric focusing (IEF) was used to screen serum for the presence of variant TTR protein following published protocols (5). Direct DNA sequencing was performed to screen the four exons of the *TTR* gene for mutations. PCR product of exon 3 was cloned into pCR 2.1 vector using a TA Cloning Kit (Invitrogen) to ascertain the heterozygous nature of the mutation. Mutation nomenclature was based on the *TTR* transcript reference (NCBI RefSeqcDNA accession number NM_000371.3). Nucleotides were numbered according to the cDNA sequence, with the first nucleotide corresponding to A of the ATG

www.pnas.org/cgi/doi/10.1073/pnas.1802977115

translation initiation codon, as specified by Human Genome Variation Society guidelines (http://varnomen.hgvs.org/).

Serum TTR concentrations were measured at Pathology Department, Boston Medical Center using a clinically-approved immunoturbidimetric assay for prealbumin (reference range 18-45 mg/dL) with coefficients of variation under 5.5% (Abbott Laboratories, Abbott Park, IL).

Site-Directed Mutagenesis and Expression and Purification of Recombinant Proteins

A synthetic human TTR gene containing an altered codon used for expression in *E. coli*, which was cloned into the pQE30 plasmid (Qiagen) as previously described (6), was used to construct the Glu51_Ser52dup TTR variant. The cDNA was modified by site-directed mutagenesis (QuikChange II Site-Directed Mutagenesis Kit, Agilent Technologies) to implement the insertion of six nucleotides at positions 212-217 encoding for two amino acids, Glu and Ser. The sequence of the forward mutagenic primer was as follows, with the bolded and underlined letters indicating the mutation site (reverse primer was the reverse complement of the forward primer): 5'-CCGGTAAAACCTCCGAATCC**GAATCC**GGTGAACTGCACGG-3'.

DNA sequencing of the complete coding region in the expression plasmid, termed rGlu51_Ser52dup TTR/pQ30, was performed to verify that the correct insertion was present. Alignment of DNA sequences for WT and Glu51_Ser52dup TTR is shown in Figure 1E.

The rGlu51_Ser52dup TTR/pQE30 expression plasmid was introduced into *E. coli* M15 [pREP4] cells by heat shock. Recombinant Glu51_Ser52dup TTR, as well as wild type (WT) and Leu55Pro TTR variant, were expressed and purified as described previously (6). Protein identity was confirmed by using electrospray ionization mass spectrometry that showed a protein mass of 13,978 Da corresponding to Glu51_Ser52dup TTR.

Prior to use, the protein solutions were dialyzed against 10 mM Na phosphate buffer, pH 7.4, 1 mM EDTA, which was a standard buffer used throughout this study.

Biophysical and Biochemical Studies of Recombinant TTR

To determine the effects of diflunisal on the TTR stability and proteolysis (Fig. 4, 5, 7 and S3), a stock solution of diflunisal (MP Biomedicals, USA) was prepared by dissolving it in DMSO, followed by a gradual dilution in ethanol and then in deionized water to the stock concentrations of 3.6 mM diflunisal, 0.1% DMSO, 9.9% ethanol. Protein solutions containing 0.2 mg/mL TTR

(14.4 μM TTR monomer) were pre-incubated with 0.36 mM diflunisal (which mimics the maximal therapeutic levels of diflunisal) for 2 hours at room temperature prior to further studies.

For studies of the effects of mutations and diflunisal on TTR oligomerization (Fig. 4A), protein samples either with or without diflunisal (14.4 mM TTR monomer, 0.36 mM diflunisal) were incubated in glass vials using Isotemp incubator (Fisher Scienific, USA) at 80 °C with shaking at 250 rpm for up to 24 hours (time 24 h, Fig. 4A). Fresh samples were used as controls (time 0 h, Fig 4A). Prior to gel electrophoresis, 20 μL sample aliquots were cross-linked with 5 μL of 25% glutaraldehyde for 4 min at room temperature; the reaction was quenched with 5 μL of 7% $NaBH_4$ in 0.1 M NaOH.

Samples were analyzed on SDS-PAGE using 16% Tricine gel (Invitrogen) developed with Gel Code Blue Stain Reagent (Thermo Scientific, USA).

Fluorescence emission spectra were recorded using TECAN Infinite M1000 PRO microplate reader (TECAN, Austria). Samples were placed in Costar 96-well black flat-bottom plates covered with clear sealing film and incubated at 37 °C with double-orbital shaking at 168 rpm. Top fluorescence signal was recorded. All measurements were done in technical triplicates.

To monitor the time course of protein chemical denaturation (Fig. 5), samples containing 0.2 mg/mL TTR were incubated for 96 hours at 25 °C in buffer solutions containing 0-4 M urea and 1 mM DTT. Tryptophan emission spectra were recorded at 315 – 390 nm with excitation at 295 nm. The ratio of the fluorescence intensity at 355 nm and 335 nm, I_{355}/I_{335}, which increases upon increasing solvent exposure of Trp, was used as a structural probe.

For equilibrium chemical denaturation, 0.2 mg/ml TTR was pre-incubated with 0-6 M urea for 96 hours. Fluorescence intensity ratio I_{355}/I_{335} (Fig. 2F) and far-UV circular dichroism (CD) at 220 nm (Fig. 2E) were recorded as a function of urea concentration to monitor changes in Trp exposure and in the secondary structure, respectively, during protein unfolding.

CD spectra, melting and kinetic temperature-jump data were recorded by using an AVIV 450 (AVIV Biomedical, NJ, USA) or a Jasco J-815 (Jasco Inc., Japan) spectropolarimeters equipped with thermoelectric temperature controllers. Secondary structure was assessed by far-UV CD spectra recorded at 190-250 nm from samples containing 0.2 mg/ml TTR placed in 1 mm quartz cells. Melting data were recorded at 215 nm to monitor β-sheet unfolding during sample heating from 25 °C to 98 °C at a constant rate of 6 °C/h. The apparent melting temperature, $T_{m\ app}$, was determined from the first derivative maximum in the melting data. Tertiary structure was assessed by near-UV CD spectra recorded at 250-300 nm from samples containing 0.6 mg/ml protein

placed in 10 mm quartz cells. In temperature-jump experiments, the sample was rapidly heated at time t=0 from 25 °C to 80 °C to trigger protein unfolding, and the time course of Trp exposure upon unfolding at 80 °C was monitored by CD at 291 nm for over 12 hours. The data were normalized to protein concentration and expressed in units of molar residue ellipticity (MRE) for far-UV CD or molar ellipticity (ME) for near-UV CD.

For limited proteolysis (Fig. 7), samples containing 1 mg/mL TTR were digested at 37 °C with trypsin at a trypsin:TTR weight ratio of 1:200. Similar diflunisal-containing protein samples were pre-incubated at 25:1 molar ratio of diflunisal:TTR monomer for 2 hours at room temperature prior to proteolysis. The reaction was quenched at various times using 1 mM phenylmethylsulfonyl fluoride. The proteolytic products were subjected to SDS-PAGE and mass spectrometry analysis.

In each mass spectrometry analysis, protein was injected onto a self-packed reversed phase column (1/32" O.D. x 500 um I.D., 5 cm of POROS 50R2 resin). After desalting for four minutes, protein was eluted with an HPLC gradient (0-100% B in 1 minute, A=0.2M acetic acid in water, B=0.2 M acetic acid in acetonitrile, flow rate ~ 30 µL/min) into an LTQ ion trap mass spectrometer (ThermoFisher Scientific, San Jose, CA) that acquired profile MS spectra (m/z 300-2000). Mass spectra were deconvoluted using MagTran1.03b2 software.

Formation of amyloid-like structure was monitored by thioflavine-T (ThT) binding / fluorescence using TECAN microplate reader. The samples containing 1 mg/mL TTR and 10 µM ThT were subjected to double-orbital shaking at 37 °C; ThT emission (λ_{ex} = 450 nm, λ_{em} = 482 nm) was recorded at 10 min intervals for 20 h. The emission of ThT in buffer alone was subtracted from the data. All experiments were performed in triplicates.

For negative stain transmission electron microscopy, a 4 µl drop containing ~0.1 mg/ml TTR was deposited onto an EM grid. The grids were stained with 1% uranyl acetate and blotted as previously described (7). Electron micrographs were collected at a 56,000 magnification using a CM12 transmission electron microscope (Philips Electron Optics, the Netherlands) equipped with a Teitz 2Kx2K CCD camera (TVIPS, Germany).

Isothermal titration calorimetry (ITC) by using a MicroCal VP-ITC (Malvern Instruments Ltd) was employed to quantify the binding of diflunisal to WT and Glu51_Ser52dup TTR. At 25 °C and a stir speed of 307 rpm, ~1 mM diflunisal in a 50% PBS buffer with 1 mM EDTA, 1% ethanol, and 0.045% DMSO was titrated into the cell containing ~100 µM TTR in the same buffer. An initial injection of 2.5 µl was followed by 50 injections of 5 µl. The last point was subtracted as a proxy for the blank and the peaks were integrated to obtain the final thermogram. The data were

approximated by using either a two-site or a single-site binding model. In addition, ITC data were recorded by dissolving diflunisal in 12% ethanol following published protocols (8); however, the high baseline level (Fig. S2 below) precluded accurate data analysis. MicroCal Origin software was used for the data analysis and display.

All experiments in this study were repeated at least in triplicates to ensure reproducibility.

Bioninformatics Analysis

We used on-line server PASTA2 (9), one of the most reliable currently available sequence-based approaches to predict amyloidogenic segments in proteins (10). The PASTA2 energy function, which was derived based on a large data set of globular proteins, reflects the stability of putative β-sheet pairings between different sequence stretches. The server provides additional information to complement the aggregation data, such as intrinsic disorder and secondary structure predictions, which was also used in the current study.

A

Probability Legend:
over 95%
80% to 94%
50% to 79%
20% to 49%
0% to 19%

Bio View:
Identified Proteins (10/14)
Including 0 Decoys

#	Visible?	Starred?		Accession Number	Molecular Weight	Protein Grouping Ambiguity	BioSample 1	BioSample 2
1	☑	★	Transthyretin variant p51-52.dup	p.51-52dup	15 kDa	★	27	17
2	☑	★	serum amyloid P-component pre...	NP_001630.1	25 kDa		9	7
3	☑	★	apolipoprotein E precursor [Homo...	NP_000032.1	36 kDa		6	5
4	☑	☆	collagen alpha-1(I) chain preprop...	NP_000079.2	139 kDa		38	37
5	☑	☆	collagen alpha-2(I) chain precurs...	NP_000080.2	129 kDa		23	11
6	☑	☆	keratin, type II cytoskeletal 1 [H...	NP_006112.3	66 kDa		1	13
7	☑	☆	keratin, type I cytoskeletal 10 [H...	NP_000412.3	59 kDa			18
8	☑	☆	trypsin-3 isoform 4 preproprotein...	NP_001184...	26 kDa	★	10	13
9	☑	☆	keratin, type II cytoskeletal 2 epi...	NP_000414.2	65 kDa	★		6
10	☑	☆	solute carrier family 22 member ...	NP_060890.2	61 kDa		2	

B

p.51-52dup (100%), 14,917.4 Da
Transthyretin variant p51-52dup
14 exclusive unique peptides, 16 exclusive unique spectra, 27 total spectra, 95/129 amino acids (74% coverage)

GPTGTGESKC PLMVKVLDAV RGSPAINVAV HVFRKAADDT WEPFASGKTS
ESESGELHGL TTEEEFVEGI YKVEIDTKSY WKALGISPFH EHAEVVFTAN
DSGPRRYTIA ALLSPYSYST TAVVTNPKE

C

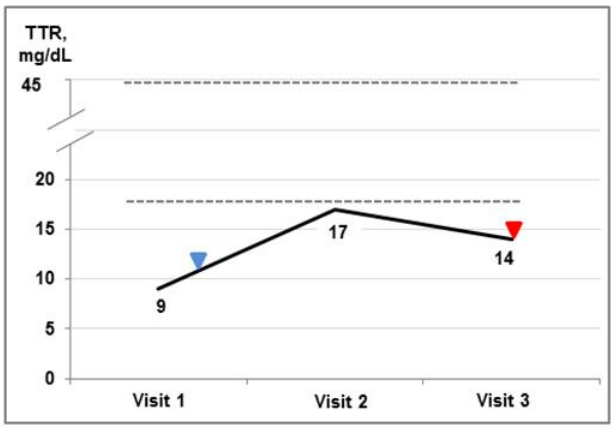

Figure S1 Proteomic detection of TTR Glu51_Ser52dup variant in amyloid deposits in skin tissue biopsy and TTR measurements in serum samples. (A) Scaffold readout of the top 10 proteins identified in Congo-red positive areas of skin tissue biopsy by laser microdissection-assisted mass spectrometry-based proteomics method. The number in the box denotes number of detected MS/MS spectra obtained from each sample for each protein. Green highlights denote >95% probability of protein identification. Blue star marks TTR; data show abundance of the TTR protein in each of two tested samples (27 and 17 spectra) and the >95% probability suggests strong confidence in the accuracy of the data. Yellow stars mark universal amyloid tissue biomarker proteins, serum amyloid P and apolipoprotein E.

(B) TTR sequence coverage demonstrated in the congophilic amyloid deposits in skin biopsy. Peptides identified by mass spectrometry-based proteomics method account for 74% of TTR sequence (shown in bold letters on yellow background). The sequence of the Glu51_Ser52dup variant is underlined. Both WT and variant peptides containing Glu51_Ser52dup were detected with comparable frequency in amyloid deposits.

(C) Serum TTR measurements at three visits. Blue and red triangles indicate the start and end of diflunisal therapy. Grey dotted lines indicate the reference range (18-45 mg/dL) for serum TTR concentration in healthy subjects.

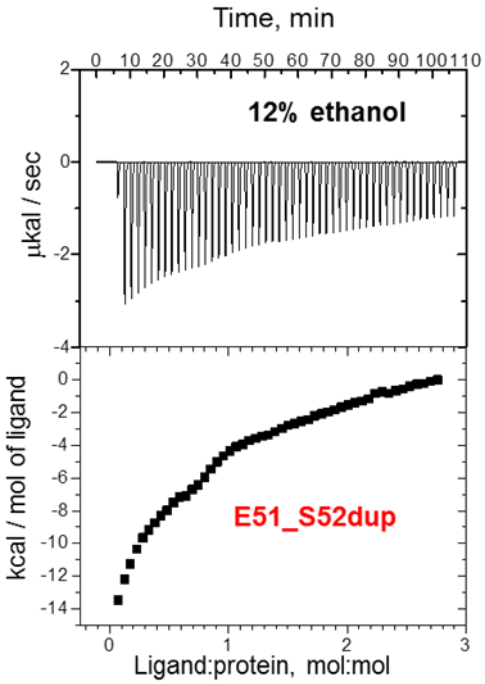

Figure S2 Isothermal titration calorimetry data recorded using diflunisal dissolved in 12% ethanol following published protocols (8). Diflunisal (1 mM) in a 50% PBS buffer with 1 mM EDTA, 12% ethanol was titrated into the cell containing ~100 µM variant TTR in the same buffer as described above in Methods. High baseline level in the data, which results from the high heat of ethanol dissolution in water, precluded accurate quantitative data analysis. To overcome this drawback, we used DMSO to dissolve diflunisal in our ITC experiments (Fig. 6).

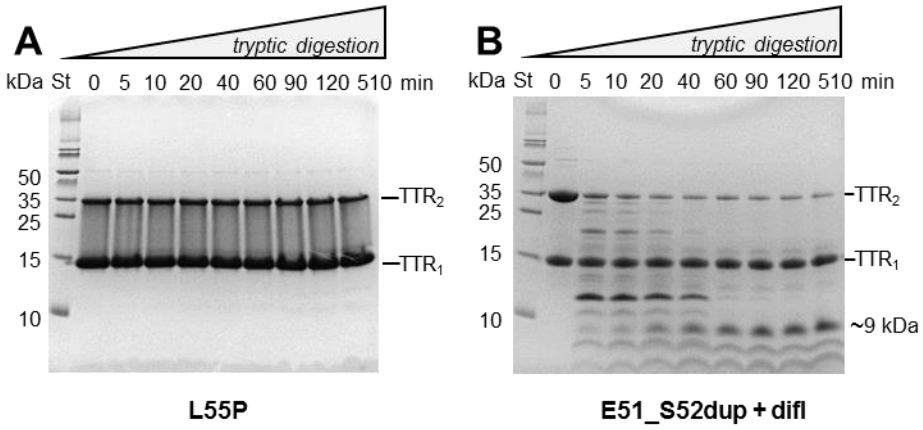

Figure S3. SDS-PAGE of TTR at various stages of tryptic digestion. TTR (1 mg/ml protein) was incubated with trypsin at 37 °C using 200:1 substrate-enzyme weight ratio. The incubation times, which ranged from 5 to 510 min, are indicated on the lanes; 0 indicates intact protein prior to incubation. TTR_1 and TTR_2 denote protein monomers and dimers, respectively. The absence of lower molecular-weight bands indicates that Leu55Pro variant was not significantly proteolyzed in these experiments (panel A), which is consistent with previous studies (11). Unlike Leu55Pro, Glu51_Ser51dup variant showed rapid proteolysis under similar conditions either in the presence of diflunisal (panel B) or in its absence (Fig. 7).

References

1. Vrana JA, Gamez JD, Madden BJ, Theis JD, Bergen HR, Dogan A (2009) Classification of amyloidosis by laser microdissection and mass spectrometry-based proteomic analysis in clinical biopsy specimens. *Blood* 114(24):4957–4959.
2. Theis JD, Dasari S, Vrana JA, Kurtin PJ, Dogan A (2013) Shotgun-proteomics-based clinical testing for diagnosis and classification of amyloidosis. *J Mass Spectrom* 48(10):1067–1077.
3. Vrana JA, Theis JD, Dasari S, Mereuta OM, Dispenzieri A, Zeldenrust SR, Gertz MA, Kurtin PJ, Grogg (2014) Clinical diagnosis and typing of systemic amyloidosis in subcutaneous fat aspirates by mass spectrometry-based proteomics. *Haematologica* 99(7):1239–1247.
4. Dasari S, Theis JD, Vrana JA, Zenka RM, Zimmermann MT, Kocher JPA, Highsmith WE, Kurtin PJ, Dogan A (2014) Clinical proteome informatics workbench detects pathogenic mutations in hereditary amyloidoses *J Proteome Res* 13(5):2352–2358.

5. Connors LH, Ericsson T, Skare J, Jones LA, Lewis WD, Skinner M (1998) A simple screening test for variant transthyretins associated with familial transthyretin amyloidosis using isoelectric focusing *Biochim Biophys Acta - Mol Basis Dis* 1407:185–192.
6. Kingsbury JS, Klimtchuk ES, Théberge R, Costello CE, Connors LH (2007) Expression, purification, and in vitro cysteine-10 modification of native sequence recombinant human transthyretin *Protein Expr Purif* 53:370–377.
7. Jayaraman S, Gantz DL, Haupt C, Gursky O (2017) Serum amyloid A forms stable oligomers that disrupt vesicles at lysosomal pH and contribute to the pathogenesis of reactive amyloidosis *Proc Natl Acad Sci USA* 114(32):E6507-E6515.
8. Adamski-Werner SL, Palaninathan SK, Sacchettini JC, Kelly JW (2004) Diflunisal analogues stabilize the native state of transthyretin. Potent inhibition of amyloidogenesis *J Med Chem* 47:355–374.
9. Walsh I, Seno F, Tosatto SCE, Trovato A (2014) PASTA 2.0: An improved server for protein aggregation prediction. *Nucleic Acids Res* 42(W1):301–307.
10. Dovidchenko NV, Galzitskaya OV. (2015) Computational approaches to identification of aggregation sites and the mechanism of amyloid growth. *Adv Exp Med Biol* 855:213-239.
11. Mangione PP, Porcari R, Gillmore JD, Pucci P, Monti M, Porcari M, Giorgetti S, Marchese L, Raimondi S, Serpell LC, Chen W, Relini A, Marcoux J, Clatworthy IR, Taylor GW, Tennent GA, Robinson CV, Hawkins PN, Stoppini M, Wood SP, Pepys MB, Bellotti V (2014) Proteolytic cleavage of Ser52Pro variant transthyretin triggers its amyloid fibrillogenesis *Proc Natl Acad Sci USA* 111(4):1539–1544.